Early Radiometric Calibration Performances of GOES-16 Advanced Baseline Imager

Fangfang Yu*[a], Xiangqian Wu[b], Xi Shao[a], Boryana Efremova[a], Hyelim Yoo[a], Haifeng Qian[a], and Bob Iacovazzi[a]
[a]ERT, Inc.@NOAA/NESDIS/STAR, College Park, MD, USA 20735; [b]NOAA/NESDIS/STAR, College Park, MD, USA 20735

ABSTRACT

GOES-16, which was launched on 19 November 2017, is the first of the next generation of geostationary weather satellites of NOAA. The Advanced Baseline Imager (ABI) is the primary instrument and mission critical payload onboard imaging the Earth with 16 different spectral bands covering 6 visible/near-infrared (VNIR) bands and 10 infrared (IR) bands. Although the GOES-16 ABI data are currently experimental and undergoing testing, in this study we focus on reporting some preliminary assessment results of the ABI radiometric calibration performance during the post-launch test (PLT) and post-launch product tests (PLPT) period. Our results show that the ABI IR full-disk (FD) images mean brightness temperature (Tb) bias with respect to S-NPP/CrIS and Metop-B/IASI of less than 0.3K. Diurnal variation is very small with a jump of less than 0.15K occurring twice a day around satellite local noon and midnight. The ABI VNIR radiometric calibration has a mean reflectance difference to SNPP/VIIRS of less than 5% for all the 6 VNIR bands except for B02 (0.64μm), which was about 8% brighter than corresponding VIIRS data during the PLT period. It may be noted that calibration of the VNIR bands experienced instabilities associated with ground system (GS) software patch testing and data receiving site failover testing, which can be reflected with the time-series monitoring from different earth and space-based invariant targets. Validations and investigations are still ongoing to improve the ABI imagery and data quality.

Keywords: GOES-16, Advanced Baseline Imager (ABI), geostationary, radiometric calibration accuracy and validation, ray-matching, PLT, and PLPT

1. INTRODUCTION

The first NOAA next-generation geostationary (GEO) weather satellite, GOES-R was successfully launched on 19 November 2016 and became GOES-16 on 30 November 2016 when it reached the geostationary orbit. The satellite is currently parking at 89.5°W at about 35,000km above the Equator undergoing a series of instrument performance and product tests. The main payload instrument on-board is Advanced Baseline Imager (ABI), which has 16 multispectral bands covering the spectrum between 0.47μm and 13.3 μm to provide continuous data stream to provide better products for weather forecasting, natural disaster warning, numerical weather prediction, and climate and environmental monitoring[1]. This instrument is the first of the NOAA GOES satellites to be fitted with a solar diffuser and a temperature-controlled blackbody to provide accurate on-orbit radiometric calibrations for the 6 visible and near-infrared (VNIR) bands and 10 infrared (IR) bands, respectively.

The ABI instrument successfully passed the Beta Maturity Peer-Stakeholder Product Validation Review (PS-PVR) on 28 February 2017 and entered the Post-Launch Product Tests (PLPT) phase the next day. During the PLPT period, a suite of planned methods and tools was applied to the ABI Instrument Calibration Level-1b (L1b) data and the associated data by the GOES-R Calibration and Working Group (CWG) at NOAA/STAR for the purpose of radiance validation and assessment[2]. In this study, we focus on reporting the ABI radiometric calibration performance using the space-based measurements, including the satellite sensor-to-sensor inter-calibrations with the measurements from the LOW-Earth-Orbit (LEO) satellites, lunar observation assessments, and ABI desert target reflectance monitoring.

*Fangfang.Yu@@noaa.gov; phone 1 301 683-2555

Earth Observing Systems XXII, edited by James J. Butler, Xiaoxiong (Jack) Xiong, Xingfa Gu, Proc. of SPIE Vol. 10402, 104020S · © 2017 SPIE · CCC code: 0277-786X/17/$18 · doi: 10.1117/12.2275195

2. ABI NOMINAL SCAN MODES AND L1B DATA

During the PLT and PLPT periods, ABI collects data mainly in Mode 3 or Mode 4 with a series of special scan modes executed intertwined. Mode 3 imaging provides one Full-Disk (FD) image, three Continental US (CONUS) and 30 mesoscale (MESO) images every 15 minutes (Figure 1, from PUG[3]). Mode 4 provides a FD image every 5 minutes (Figure 2, from PUG[3]). While FD and CONUS images are scanned at fixed angles, MESO images can be collected literately any places within the Field of Regard (FOR). The MESO scan in mode 3 is therefore used to chase and scan the Moon while it appears in the space within the ABI FOR. Each MESO consists of two NS adjacent swathes. As the height of each swath is wider than the diameter of the Moon, we use one of the swaths to collect the lunar images when it transits across the space within the ABI FOR.

After the radiometric calibration, the radiance of each sample is navigated and resampled to fixed grid in each ABI Earth image. The fixed grids are a set of static pixel locations relative to an ideal geostationary satellite viewpoint and are used to aid users by providing continuity in locations of geographic, features throughout the satellite missions' life. There is no space data in the ABI fixed gridded L1B data. The NOAA GOES-R ground system (GS) processes the Earth images collected with mode 3 or mode 4 timeline into L1B format.

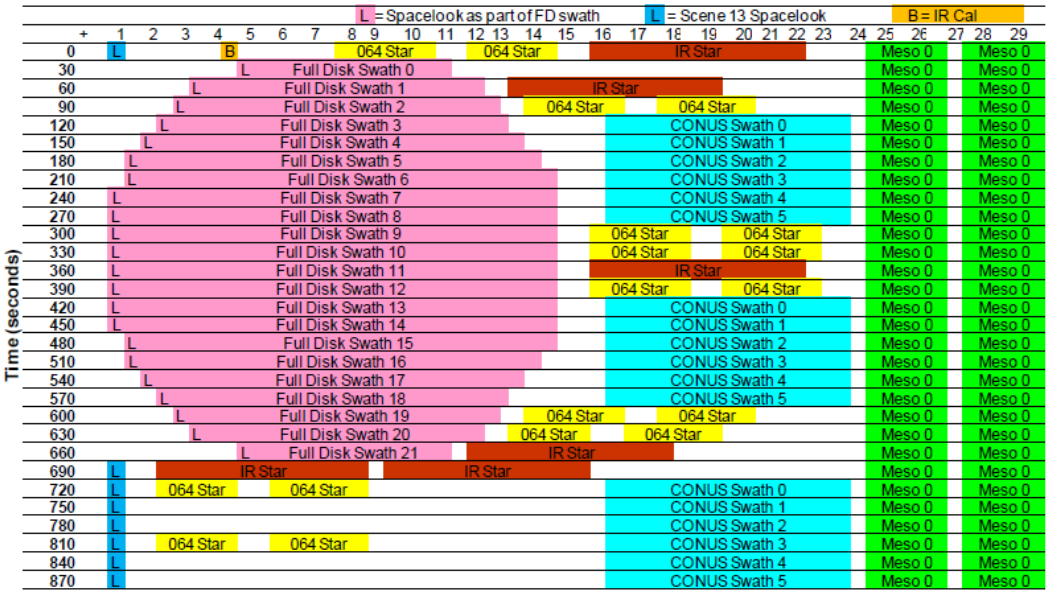

Figure 1. ABI Mode 3 timeline, from PUG[4].

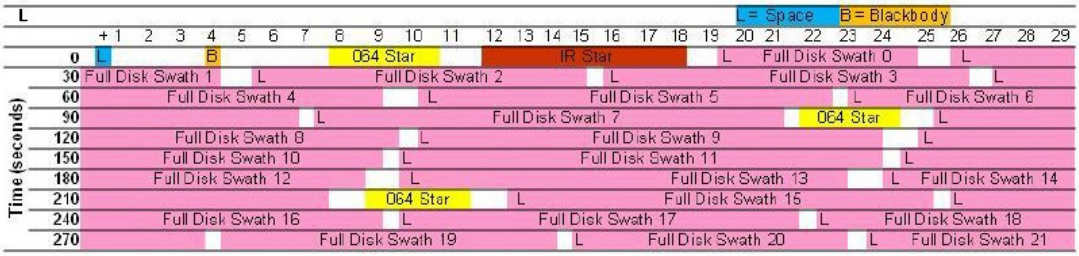

Figure 2. ABI Mode 4 timeline, from PUG[4]

3. ABI CALIBRATION

Like the Advanced Himawari Imager (AHI) onboard the Japan Meteorological Agency (JMA) Himawari-8 which was launched on October 15, 2015, ABI has two independent scan mirrors, the East-West and North-South scan mirrors, for quick repositioning with flexible and configurable custom scans. The two-point calibration

scheme with quadratic detector responsivity is used to calibrate the measured count of scan object to radiance with the contributions of reflectance/emissivity from the two scan mirrors accounted[4]. The incident angle dependent reflectivity and emissivity of the two scan-mirrors are also measured on-ground before launch. The quadratic term of each detector is also derived from pre-launch measurements, while the linear calibration term is determined on-orbit from the measurements of the two point calibration targets.

3.1 Thermal IR Calibration

The internal calibration target (ICT) of blackbody (BB) and deep space looks (SL) are the two calibration targets used to determine the linear calibration coefficients for each IR detector. The onboard BB is a temperature controlled three bounce cavity. The BB is observed at every 5 or 15 minutes depending on the scan mode selected. The space look is collected every 30 seconds for Mode 3 or every swath for Mode 4. As shown in Figure 1 and 2, for the data scanned during the FD scan time, the calibration scan look is conducted at every FD swath by extending the swath scan to the space at the dark side of the Earth. For the data collected during the 3rd CONUS period in Mode 3 timeline, the corresponding calibration space look is conducted at the space at the dark side of the Equator[5]. The angular dependence of the mirror reflectance and the emissivity of the mirrors are measured pre-launch and provided as LUTs for on-orbit radiometric data analysis to produce radiance.

The equation of the IR calibration algorithm for the linear coefficient (m) can be descripted as follows:

$$m = \frac{L_{BB} - q\Delta C_{BB}^2 + (L_{EW@BB} + L_{NS@BB}) - (L_{EW@SL} + L_{NS@SL})}{\Delta C_{BB}} \quad (1)$$

$$\Delta C_{BB} = C_{BB} - C_{SL,BB} \quad (2)$$

Where L_{BB} is the band-averaged spectral radiance at BB view, $L_{EW@BB}$ and $L_{NS@BB}$ are spectral radiance contributed from the EW and NS scan mirrors, respectively at BB view. C_{BB} is the measured count at BB view and $C_{SL,BB}$ is the count of the BB calibration space look conducted right before BB view.

The linear coefficient (m) is updated every BB view. The scene radiance of the earth target L_{ev} can be determined as follows:

$$L_{ev} = \frac{m\Delta C_{ev} + q\Delta C_{ev}^2 - (L_{NS@ev} - L_{NS@SL}) - (L_{EW@ev} - L_{EW@SL})}{\rho_{NS@ev}\rho_{EW@ev}} \quad (3)$$

$$\Delta C_{ev} = C_{ev} - C_{SL} \quad (4)$$

Where $L_{EW@ev}$ and $L_{EW@SL}$ are spectral radiance contributed from the EW mirror at Earth view and space look view, respectively. $L_{NS@ev}$ and $L_{NS@SL}$ are spectral radiance contributed from the NS mirror at Earth view and space look view, respectively. $\rho_{EW@ev}$ and $\rho_{NS@ev}$ are the reflectance of the EW and NS scan mirrors at the angles as they view the earth scene target. C_{ev} is the earth scene count and C_{SL} is the space look count before earth target scan.

3.2 VNIR Calibration

A Spectralon™ solar diffuser (SD) and the deep space looks (LS) are used for the calibration of VNIR bands. The solar calibration is scheduled as needed. It was conducted at higher frequency in the early in-orbit stage and gradually reduced as time going-by as the instrument degrades stably. Again the quadratic coefficient for each detector is determined on ground and the linear term (m) is calculated and updated based on in-orbit measurements of the two calibration targets. The calibration equation and earth scene radiance calculation follow from Equation (1)-(4) except that the mirror emissivity contributions are negligible.

$$m = \frac{f_{\text{int}} L_{SD}^{eff} - q(C_{SD} - C_{SL,SD})^2}{(C_{SD} - C_{SL,SD})} \qquad (5)$$

Where f_{int} is the integration factor for viewing SD. It is set to 9x for all the ABI VNIR bands during the PLPT period. C_{SD} and $C_{SL,SD}$ are the counts at SD view and the solar calibration space look with the same integration time as SD view, respectively. L_{SD}^{eff} is the spectral radiance received by the detector at SD view.

$$L_{SD}^{eff} = L_{SD} \rho_{NS@SD} \rho_{EW@SD} \qquad (6)$$

Where $\rho_{NS@SD}$ and $\rho_{EW@SD}$ are the mirror reflectivity at SD view. L_{SD} is the SD spectral radiance at the sun and detector viewing geometries.

$$L_{SD} = K_{\beta_{eff}}^{\text{det}ector\_Row\#} \cos(\theta_{sun}) \left[\pi L_{100\%\alpha} (\frac{R_{sun}}{r_{sun}})^2 \right] \qquad (7)$$

Where $K_{\beta_{eff}}^{\text{det}ector\_row\#}$ is the factor to account for the SD BRDF impact at solar and detector viewing geometry which is measured pre-launch, θ_{sun} is the sun incidence angle, R_{sun} is the average radial distance from Earth to the Sun (i.e. 1 AU) and r_{sun} is the actual distance between the Earth and the Sm at SD view time, $L_{100\%a}$ is the spectral solar irradiance at 1AU over a Lambertian surface with 100% albedo. Therefore the factor $\cos(\theta_{sun}) \left[\pi L_{100\%\alpha} (\frac{R_{sun}}{r_{sun}})^2 \right]$ is the solar irradiance normal to the solar diffuser surface at the solar incidence angle of θ_{sun} and the sun-earth distance of r_{sun}.

The earth scene radiance for the VNIR bands is calculated as:

$$L_{ev} = \frac{m(C_{ev} - C_{SL}) + q(C_{ev} - C_{SL})^2}{\rho_{NS@ev} \rho_{EW@ev}} \qquad (8)$$

Where C_{ev} is measured count at earth scene, C_{SL} is normal deep space count, and $\rho_{NS@ev}$ and $\rho_{EW@ev}$ are the mirror reflectivity at earth scene angles.

4. ABI IR RADIOMETRIC CALIBRATION ACCURACY VALIDATIONS

Two well-calibrated hyperspectral radiometric instruments onboard at LEO satellites, SNPP Cross-track Infrared Sounder (CrIS) and Metop-B Infrared Atmospheric Sounding Interferometer (IASI), are used as the reference instruments to validate the GOES-16 ABI IR radiometric calibration accuracy. The GEO-LEO IR inter-calibration was conducted following the standard procedure developed by the Global Space-based Inter-Calibration System (GSICS) community[6, 7]. The spatially, temporarily and spectrally matched scenes observed with similar viewing zenith angles are routinely identified and archived for the ABI full-disk scan images since the first light of ABI. As the cloud can be moving during the time interval between the satellite observations, a set of uniformity criteria are applied to each ABI IR band to ensure that both GEO and LEO observe the same targets. This uniformity criteria can also help to reduce the uncertainty caused by the navigation difference between the two satellites.

Figure 3 shows the GOES-16 ABI IR spectral response functions (SRF) and the simulated IASI and CrIS brightness temperature (Tb) over clear-sky Tropical Ocean. IASI covers all the ABI IR spectral ranges, thus we can simulate the 10 bands of ABI radiance for the collocated scenes with collocated IASI observations. However, due

to the missing and spectral gap in between the CrIS bands, only eight ABI IR bands' radiance are simulated with the collocated CrIS measurements. The radiance is not simulated with CrIS for ABI B07 (3.9μm) and B11 (8.5μm). Also be noticed that CrIS doesn't fully cover the left fail of ABI B08 (6.2μm) SRF.

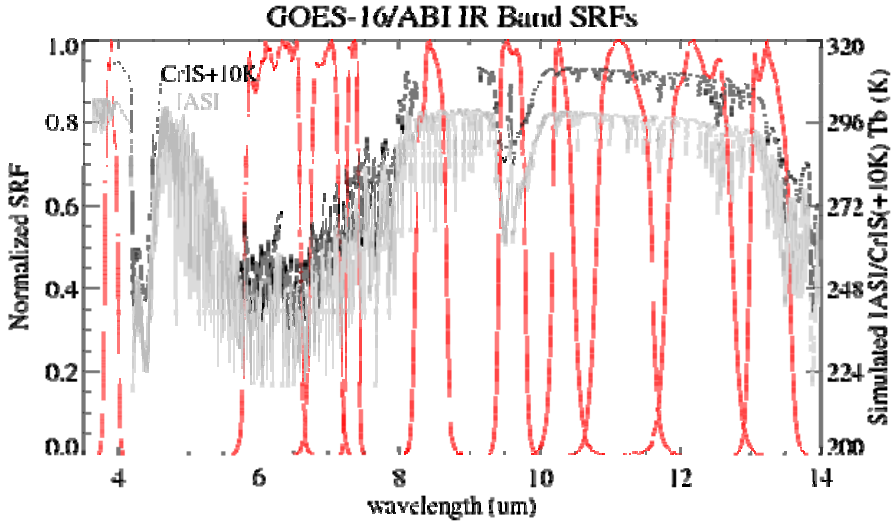

Figure 3. GOES-16 ABI IR spectral response functions (in red) and the simulated IASI (in gray) and CrIS (in black, shifted by +10K) over clear-sky Tropical Ocean.

4.1 Mean Tb Bias to CrIS/IASI

The radiance of all the GOES-16 ABI IR bands is in general well calibrated. Figure 4 displays the mean Tb bias to CrIS and IASI at both day and night collocations obtained from March 1 through 20, 2017. ABI IR data is generally slightly colder than both CrIS and IASI with the mean Tb bias less than 0.30K. The mean Tb bias difference to CrIS and IASI is within ~0.1K, which agrees with the CrIS and IASI calibration difference[8]. The slight warm Tb bias to CrIS at ABI B08 (6.2μm) is due to the missing CrIS spectra over the ABI B08 spectral range at the left tail. The day-time ABI data is slightly warmer than night-time data within 0.15K, if detectable.

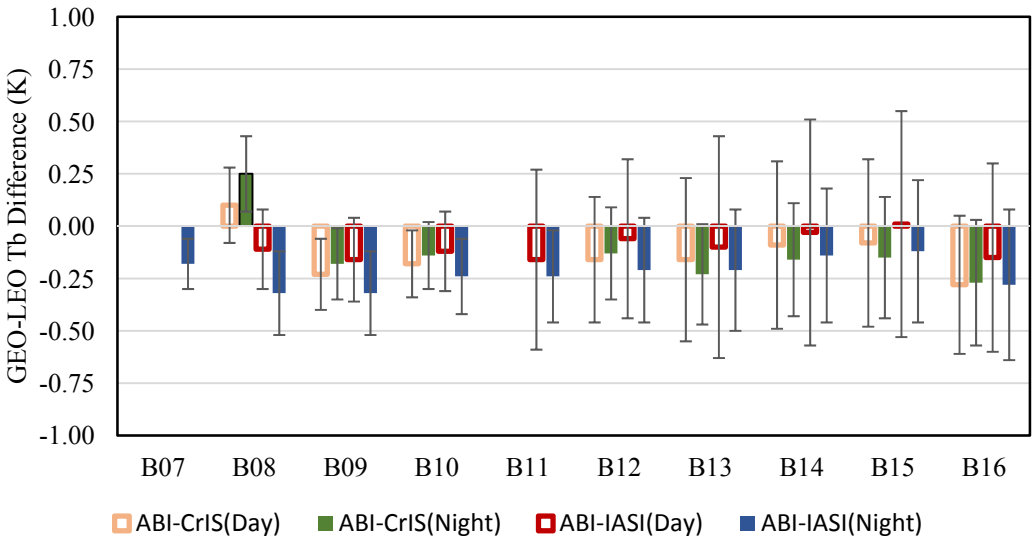

Figure 4. Mean Tb difference and the standard deviation between ABI and CrIS/IASI for the ABI FD data in March 2017.

4.2 Diurnal Variation of Tb Bias

The night-time collocations obtained from March 1 through 31, 2017 are binned at 0.5 hour time interval to examine the possible diurnal variation, following the similar method as described in Yu et al.[9]. A minimum of 400 uniform scenes is applied to ensure the robust mean Tb bias at each time bin. Both the Tb bias to CrIS and ASI showed that ABI is slightly warmer during the day-time than the night-time. A jump of about 0.10-0.2K mean Tb bias can be observed at both CrIS and IASI collocation data around the satellite midnight time (~6:00UTC) at most IR bands (Figure 3 as an example). The corresponding Tb bias was dropped around the satellite noon time (~18:00UTC). This slight changes in the Tb bias around the midnight and noon occur coincidentally with the slight change in the gain values of the IR calibration coefficients[10]. Recent investigation of the space data in the ABI lunar scan images suggested that these small but sudden changes of Tb bias is most likely caused by the non-uniformity of ABI East-West (EW) scan mirror emissivity correction[7].

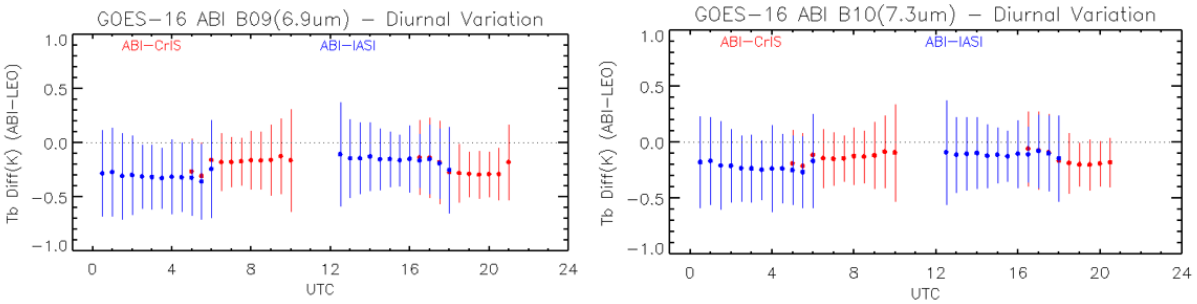

Figure 5. An example of diurnal variation in the Tb bias to CrIS and IASI for B09 and B10, showing the sudden changes in Tb bias around the satellite midnight time and noon time.

4.3 Long-term Tb bias monitoring

The long-term radiometric calibration stability is monitored with the daily mean Tb bias to the two reference instruments. As shown in Figure 6, the consistent daily mean Tb bias to CrIS/IASI since Jan. 15, 2017 indicates that ABI IR bands are well-calibrated and very stable.

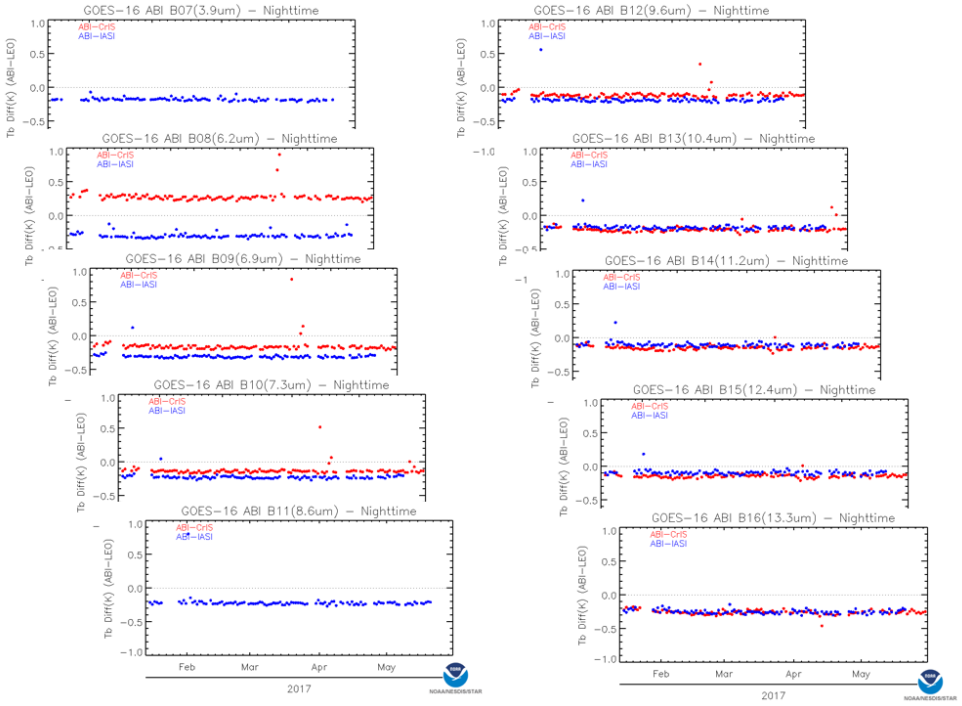

Figure 6. Time-series of daily mean Tb bias to IASI and CrIS for the night-time collocations. Investigation is needed to understand the cause to the outlies.

5. VNIR RADIOMETRIC CALIBRATION ACCURACY VALIDATION

Several methods are developed and applied to validate and monitor the radiometric calibration accuracy, including the inter-calibration with the Visible Infrared Imaging Radiometer Suite (VIRS) on-board SNPP satellite, deep-convective cloud (DCC) calibration, Rayleigh scattering for the short wavelength band, desert target reflectance monitoring and lunar trending[2]. The ray-matching method is used as the primary method to validate the radiometric calibration accuracy, desert reflectance monitoring is mainly used to validate rapid changes of the solar calibration, and the other methods are used to cross-check the results.

5.1 Initial Radiometric Calibration Accuracy with Ray-matching method

SNPP/VIIRS is used as the reference to validate the radiometric calibration accuracy of ABI VNIR bands (Figure 7). The ray-matching method provides a straight forward tool for the direct inter-comparison between GEO and LEO instruments for all-sky scenes[11]. This method was also used to validate the radiometric calibration accuracy of the Japan Meteorological Agency (JMA) Himawari-8 Advanced Himawari Imager (AHI) VNIR bands[12]. Like the GEO-LEO IR inter-calibration, this method compare the observations over the same Earth surface targets at which both GEO and LEO instruments scan with the similar viewing and illumination angles with similar atmospheric conditions. But matching in the viewing azimuth angle is additionally applied in the ray-matching method to reduce the bidirectional reflectance function (BRDF) impact. The homogeneous scenes are also used to ensure the two satellites observe the same target and compensate for the navigation difference. In this report, the SNPP VIIRS M03, I2, M7, M9, M10 and M11 are selected as the reference to characterize radiance quality for the correspondingly spectrally matched ABI bands.

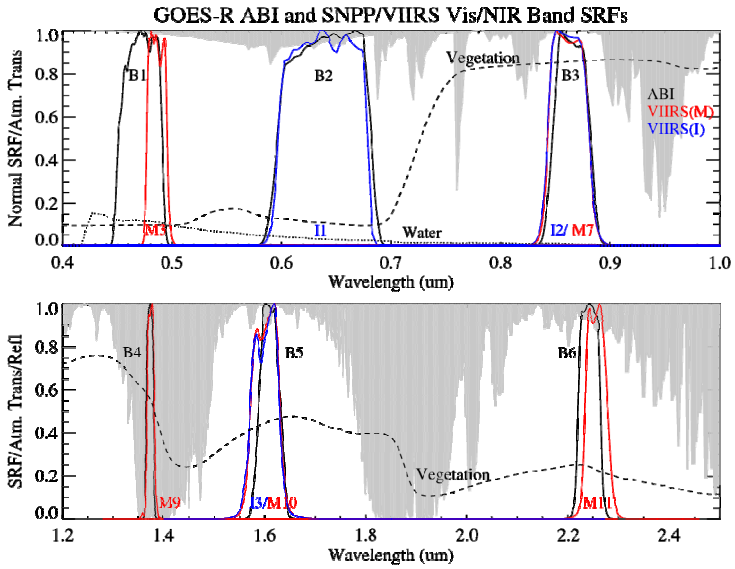

Figure 7. ABI and VIIRS SRFs, over plotted with the spectra of vegetation, water, and atmospheric transmittance.

To compensate for the ABI and VIIRS SRF difference, we use the Scanning Imaging Absorption spectrometer for Atomospheric CHartograpY (SCIAMARCHY) derived spectral band adjustment factors (SBAF) provided by NASA Langley[13]. As NOAA employs the VIIRS Non-Government (NG) version of SRFs for the operational calibration, the linear fit SBAF derived with NPP-VIIRS-NG SRF are selected from the SBAF web-tool. Unfortunately, there is SCIMARCHY-based SBAF for ABI B06 (2.3μm). We assume the SBAF value for this band is 1.0 due to the similar SRFs between ABI B06 and VIIRS M11 and there is no strong atmospheric absorption within the spectral range (Figure 7). All the inter-calibration analysis are based on the reflectance using the SBAF correction equation as follows:

$$R_{VIIRS,ABI} = \frac{R_{ABI} - SBAF_{offset}}{SBAF_{slope}} \quad (9)$$

Where R_{ABI} is the ABI reflectance and $R_{VIIRS,ABI}$ is the corresponding ABI reflectance corrected with VIIRS SRF. $SBAF_{slope}$ and $SBAF_{offset}$ are the SCIAMACHY-based linear regression coefficients, respectively.

Since the first light of ABI VNIR bands on Jan. 14, 2017, the ABI L1B data experienced several calibration anomalies for the solar reflective bands during the PLPT period. The collocation data obtained from the relative solar calibration, from Jan. 15 through February 11, 2017 are used to examine the initial calibration accuracy for the VNIR bands. To reduce the BRDF impact, the ABI and VIIRS viewing azimuth angle difference should be less than 15 degrees. The coefficients of variance (CoV) for VIIRS pixels within ABI footprint and the surrounding area should be less than 5%.

Figure 8 shows the scatterplots of the scene dependent reflectance ratio between ABI and VIIRS. Large scattering of reflectance ratio can be observed at low radiance scenes. This is because the reflectance ratio values are much more sensitive to the striping/banding and other noises at low radiance. A set of threshold values are some randomly selected to calculate the mean reflectance ratio for each bands (Table 1). Only the scenes with reflectance greater than the thresholds are used to calculate the reflectance ratio between ABI and VIIRS and reported in Table 1. No apparent scene dependent reflectance ratio can be observed at the scenes at mid- and high- reflectance scenes. As reported in Table 1, the initial solar calibration accuracy is within 5% difference from VIIRS for B01 (0.47μm), B03 (0.87μm), B04 (1.38μm), B05 (1.61μm) and B06 (2.25μm). The mean reflectance ABI B02 (0.64μm) is 8.1% brighter than VIIRS I02 (0.64μm). It was reported that ABI B02 initial solar calibration coefficients were also about 7-8% larger than the pre-launch value[14]. Root cause to the large difference is unknown yet and will be investigated in the soon future.

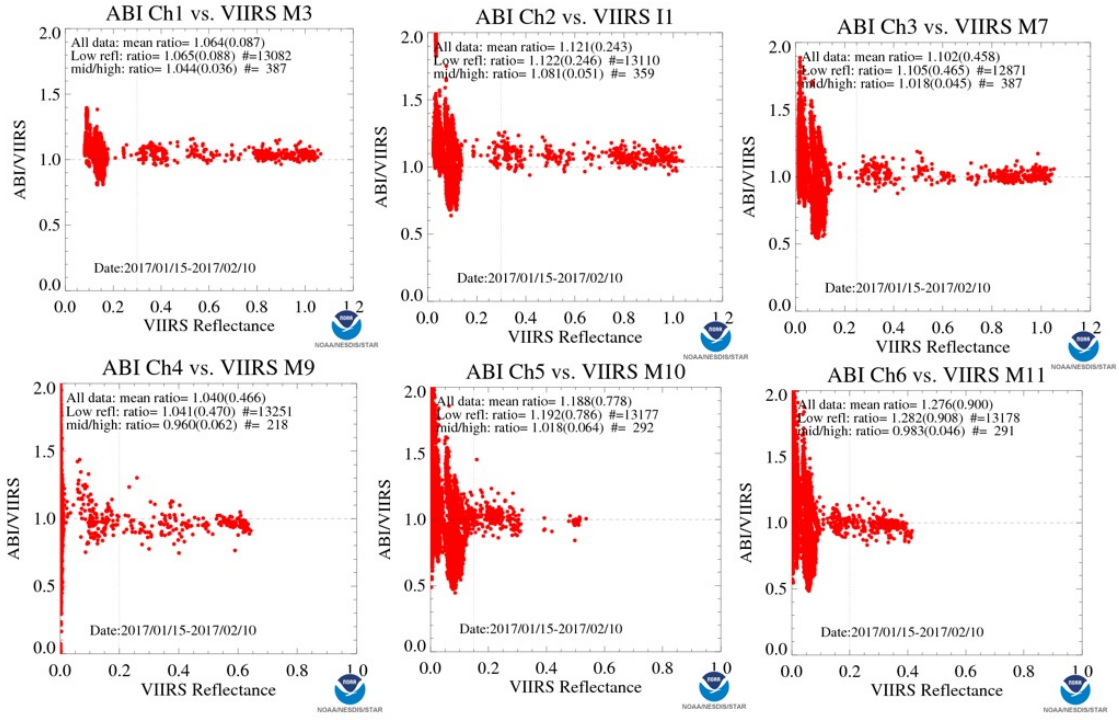

Figure 8. Scatterplots of the reflectance ratio between ABI and VIIRS for the collections collected between Jan. 15 through Feb. 11, 2017.

Table 1. Reflectance thresholds and the reflectance ratios for the mid- and high- reflectance scenes.

		B01 (0.47μm)	B02 (0.64μm)	B03 (0.87μm)	B04 (1.38μm)	B05 (1.61μm)	B06 (2.25μm)
Reflectance ratio	Mean	1.044	1.081	1.018	0.960	1.018	0.983
	Standard Deviation	0.036	0.051	0.045	0.062	0.064	0.046
	Collocation#	387	359	387	218	292	291
Reflectance Threshold		0.25	0.25	0.25	0.20	0.10	0.10

5.2 VNIR calibration stability

The ABI and VIIRS collocation data along the Equator in between 17:00-20:00 UTC period are routinely generated and archived since the ABI first light for the VNIR bands. As we use the reflectance ratio to characterize the calibration difference between the two instruments, only mid- and high- reflectance scenes are used to validate the to avoid of large uncertainty at low radiance scenes. Unfortunately, the GOES-16 sub-satellite point region is dominated with ocean with low cloud coverage. To achieve sufficient collocations for the daily monitoring, we relax the criteria to select the uniform targets and viewing geometric match-ups, that is, the coefficients of variance for VIIRS pixels within ABI footprint and the surrounding area is less than 10% and the viewing azimuth difference between ABI and VIIRS should be less than 30 degree with a minimum of 100 pixels.

Figure 9 shows the daily mean ABI and VIIRS reflectance ratio. The trending of both methods shows that ABI solar calibration is not quite stable during the study period. Several anomalies were reflected in the figure, including the calibration anomalies between Feb 12 -17, March 15 – April 28, June 10-12. The root cause to the anomaly in between March 15 – April 28 has been found and it was caused by mis-implementing the look-up-table derived with incorrect integration time for the solar calibration[15]. Root causes to the other ones are unknown yet. The ABI solar calibration accuracy is also monitored with daily reflectance at Sonoran and Uyuni deserts and the lunar data during the PLPT period[16,17].

6. SUMMARY

GOES-16 ABI is the most advanced geostationary weather instrument NOAA has ever developed. It has not been declared operational and its data are still preliminary and undergoing testing. In this study, we reported some preliminary validation results of the early ABI radiometric calibration performance during the PLT/PLPT periods, including the radiometric calibration accuracy at different temporal scales and the spatial uniformity of the scan mirrors for the VNIR and IR bands. The ABI IR bands are well calibrated and stable with the mean Tb bias to CrIS/IASI measurements at less than 0.3K with small diurnal variation occurred around the satellite midnight and noon time. Users reported the periodic infrared calibration anomaly (PICA) between the FD/CONUS/MESO images. Recent assessments of the lunar chasing images indicated that the root causes to the PICA and diurnal variations are most likely associated with the possible non-uniform corrections of the incident-angle dependent emissivity of the NS and EW scan mirrors. Further investigation is undergoing to confirm and then correct the anomalies.

The radiometric calibration accuracy of the VNIR bands were good at the beginning of the PLT/PLPT periods. The mean reflectance difference to SNPP/VIIRS was within 5% for ABI VNIR bands except for B02 which was about 8% brighter than VIIRS. The ABI B02 initial solar calibration coefficients were also about 7-8% larger than the pre-launch value. Further investigation is needed to understand the root causes to the larger on-board calibration coefficients. ABI VNIR radiometric calibration was not very stable during the PLPT period due to software patch testing and data receiving site failover testing. Different vicarious methods using different invariant targets are being applied to monitor the radiometric calibration stability and trending. The CWG team is continuing the effort to better understand the ABI calibration performance and improve the data quality.

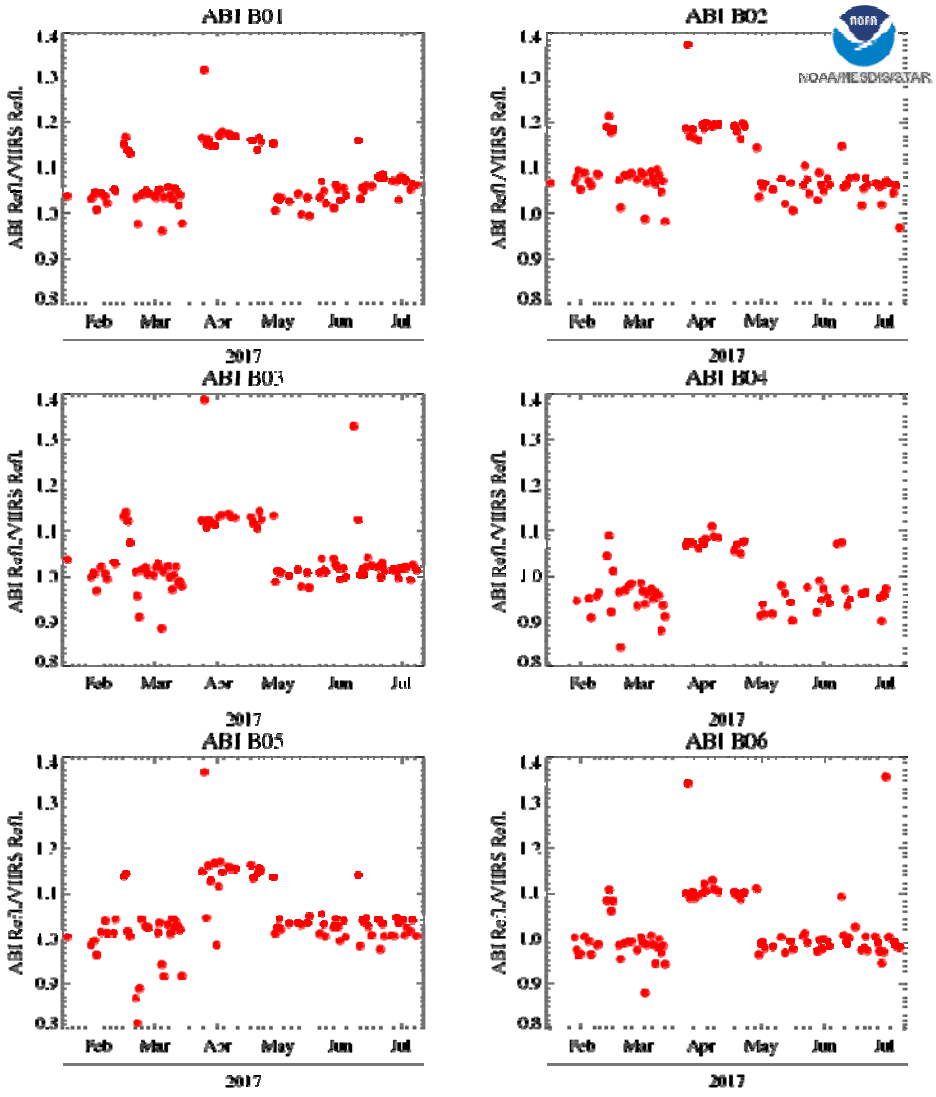

Figure 9. Time-series of daily reflectance ratio between ABI and VIIRS.

ACKNOWLEDGEMENTS

This work is supported by NOAA GOES-R project. This manuscript content is solely the opinions of the authors and do not constitute a statement of policy, decision, or position on behalf of NOAA or the U.S. government. GOES-16 satellite has not been declared operational and its data are preliminary and undergoing testing.

REFERENCES

[1] Schmit, T., Gunshor, M., Menzel, W.P., Gurka, J., Li, J. and Bachmeier, A.S., "Introducing the next-generation Advanced Baseline Imager on GOES-R," Bulletin of the American Meteorological Society, 1079-1096 (2005), doi:10.1175/BAMS-86-8-1079.

[2] NOAA GOES-R Series ABI Beta, Provisional and Full Validation Readiness, Implementation and Management Plan (RIMP), 416-R-RIMP-0315, Version 1.1, July 2016.
[3] Product Definition and Users' Guide (PUG), Vol 3: Level1B Products for GOES-R Series Core Ground Segment, Harris Corporation, Revision D, May (2015).
[4] Datla, R., Shao, X., Cao, C. and X. Wu, "Comparison of the calibration aglorithms and SI traceability of MODIS, VIIRS, GOES and GOES-R ABI sensors," Remote Sensing, 8(126) (2016), doi:10.3390/rs8020126.
[5] Yu, F. et al., GOES-R Calibration Working Group Report, College Park, Maryland, June (2017).
[6] Wu,X., Hewison, T. and Tahara, Y., "GSICS GEO-LEO inter-calibration baseline algorithm and early result", Proc. SPIE, San Diego, CA, (2009).
[7] Hewison, T., Wu, X., Yu, F., Tahara, Y., Hu, X., Kim, D. and M. Koeing, "GSICS iner-calibration of infrared channels of geostationary imagers using Metop/IASI," IEEE Geosci. Remote Sens. 51, 1160-1170 (2013).
[8] Wang, L., Han, Y., Jin, X., Chen, Y. and D.A. Tremblay, "Radiometric consistency assessment of hyperspectral infrared sounders,", Atmo. Meas. Tech., 8, 4831-4844 (2015).
[9] Yu, F., Wu, X., Rama Vara Raja, M. K., Li, Y., Wang, L. and M. Goldberg, "Evaluation of diurnal calibration variation and scan angle emissivity calibration for GOES Imager infrared channels," IEEE Trans., Geosci. Remote Sens. 51(1) 671-683 (2013).
[10] Efrovema, B. et al., GOES-R Calibration Working Group report, College Park, Maryland, March (2017)
[11] Doelling, D., Minnis, P. and L. Nguyen, "Calibration comparison between SEVERI, MODIS and GOES data," Proc. Of MSG RAO Workshop, Salzurg, Austria, Sept. (2004).
[12] Yu, F. and X. Wu, "Radiometric inter-calibration between Himawari-8 AHI and S-NPP VIIRS for the solar reflective bands," Remote Sensing, 8, 270-285 (2016).
[13] Scarino, B., Doelling, D., Minnis, P., Gopalan, A., Chee, T., Bhatt, R., Lukashin, C. and C. Haney, "A web-based tool for calculating spectral band difference adjustment factors derived from SCIAMAHY hyper-spectral data," IEEE Trans. Geosc. Remote Sens. (2016).
[14] Efrovema, B. GOES-R Calibration Working Group report, College Park, Maryland, February (2017).
[15] Efrovema, B. GOES-R Calibration Working Group report, College Park, Maryland, April (2017).